© Indian Academy of Sciences

Stability analysis of a prey refuge predator–prey model with Allee effects

Unal Ufuktepe[1], Burcin Kulahcioglu[2] and Olcay Akman[3]*

[1]*College of Engineering & Technology, American University of the Middle East, Kuwait City, Kuwait*

[2]*Department of Mathematics, Izmir University of Economics, İzmir, Turkey*

[3]*Department of Mathematics, Illinois State University, Normal, USA*

*Corresponding author (Email, oakman@ilstu.edu)

We constructed a discrete-time predator–prey model by adding prey refuge and Allee effects (predator saturation on prey and mate limitation on predator) to an earlier prey–predator model and examined its dynamics. We show the existence of positive fixed points and study the stability properties. The numerical simulations and bifurcation diagrams verify the impact of refuge and the Allee mechanism on the system.

1. Introduction

Predator–prey interactions are one of the important study areas focused on by ecologists and mathematicians. The dynamic relationship between predators and their prey is a dominant theme especially in mathematical ecology due to its universal applicability and importance. Traditionally, most common studies in this arena focus on the dynamics of a predator–prey system under varying effects and parameters. Allee effects and hiding behavior of prey on the dynamics of predator–prey interactions represent an important portion of these studies. The hiding behavior of prey and its impact on the predator–prey system have been studied by numerous researchers, including Hassell and May (1973) and Hassell (1978).

The prey refuge effect is a mechanism caused by heterogeneity in the environment. It refers to the fact that some prey can be sheltered from danger or can be inaccessible to predators. The refuge effect has been studied widely by McNair (1986); Jana (2013). This effect contributes positive feedback to the growth of prey while having a negative impact on predators. The studies indicate that the effect of refuge used by the prey has a substantial effect on the coexistence of prey and predator, in that it increases the equilibrium density of prey population, and stabilizes the positive fixed point of the system.

Some studies on the prey refuge effect show that this effect either decreases with increasing prey density, or increases with both predator and prey density, and the addition of prey refuge substantially reduces the risk of prey extinction (Taylor 1984; Ma *et al.* 2009). However, it also plays a destabilizing role under a very restricted set of conditions (Ma *et al.* 2009).

The Allee effect is an important concept that may be added to population models in order to make them more realistic. In one-dimensional models with the Allee effect, there is a positive relationship between the growth rate and population size at low densities due to cooperation. On the other hand, at high densities, competition is more dominant than cooperation, so the Allee effect begins to lose its impact. As a result, the relationship reverses itself at high densities. Considering the Allee effect is important in understanding why some populations get smaller and even face extinction. Depending on the models used, the Allee effect may cause a stabilizing (Scheuring 1999) or destabilizing effect (Wang *et al.* 1999).

In this article, we consider the prey refuge and Allee effects on predator–prey interaction by using both analytic and numerical approaches. We construct a model that contains a predator saturation term. The refuge effect is commonly considered to act on a fixed proportion of the prey population; our approach provides an extended model to study the dynamics of the predator–prey interaction under various different refuge settings.

The model previously considered by Celik and Duman (2009) and Ufuktepe *et al.* (2013), which includes neither the Allee effect nor the prey refuge effect, is given by

$$N_{t+1} = N_t + rN_t(1 - N_t) - aN_tP_t$$
$$P_{t+1} = P_t + aP_t(N_t - P_t), \tag{1}$$

where N_t and P_t are the densities of the prey and predator population at time t respectively. The growth parameter r and the predation parameter a are both positive. Adding prey refuge to (1) results in the following model (Rana *et al.* 2014):

$$N_{t+1} = N_t + rN_t(1 - N_t) - (1 - d)aN_tP_t$$
$$P_{t+1} = P_t + aP_t((1 - d)N_t - P_t), \tag{2}$$

where $d \in [0, 1)$ is the proportion of prey that is not available to the predator because of the refuge effect. It is important to mention that system (2) allows for prey reproduction while in refuge. For certain types of animals, this may not be the case.

We now examine the dynamics of models under the Allee effect.

2.   Mechanisms of the Allee effect

The Allee effect depends on the concepts of cooperation and the cost of rarity. It is a causal positive relationship between the number of individuals in a population and their overall individual fitness. If the population is too small, then foraging, hunting, finding mates for reproduction, or protection becomes more difficult for individuals. As a result, when the population is small, a positive relationship between the population size and the growth should be expected.

Generally, Allee effects are classified into two categories:

(i)   Allee effects caused by predator saturation, and
(ii)   Allee effects caused by mate limitation.

Predator saturation causes an increase in individual prey vulnerability, as prey population gets sparser. This mechanism is observed in many species, including colonial seabirds, synchronously emerging insects, island fox and American toad (Courchamp *et al.* 2008). In this study, we add the predator saturation to the model as follows.

First, let us consider the probability of escaping from the predator with a saturating functional response: $A(N) = \exp(-\beta/(1 + sN))$, where β is the predation intensity and s is proportional to the handling time, as shown in Schreiber (2003). Here, the handling time can be considered as a function of the time spent in pursuing, hunting, eating and digesting prey. On the other hand, the predation intensity β depends on the distance between species, their speeds and the proportion of successful attacks (Hassell *et al.* 1976).

Mate limitation is probably the most observable mechanism of the Allee effect. Cod, gypsy moth, alpine marmot and Glanville fritillary butterfly are some species facing a mate limitation effect (Courchamp *et al.* 2008). The formula

$Q(N) = N/(m + N)$ is used for the probability of finding a mate, where $1/m$ is an individual' searching efficiency. We add this effect to the predator, so we use $Q(P) = P/(m + P)$.

3.   The model

We now extend the model given in (2) by adding a new predator saturation term to the prey population, as well as mate limitation of the predator. This results in the following system:

$$N_{t+1} = N_t + rN_t(1 - N_t)e^{-(\beta/1 + sN_t)} - (1 - d)aN_tP_t$$
$$P_{t+1} = P_t + aP_t((1 - d)N_t - P_t)\left(\frac{P_t}{m + P_t}\right), \tag{3}$$

where all parameters are positive. Model (3) is a realistic one since some proportion of prey is less vulnerable to being attacked due to sheltering. The environment is often not homogeneous, and the refuge effect introduces spatial heterogeneity to the population. Moreover, some of the prey can escape from their predators not because of sheltering but due to predator saturation. This is included in (3) as an Allee effect. In addition, the predator may face difficulty in finding mates at low densities, and this Allee effect plays an additional role in (3).

We obtain the fixed points (0, 0), (1, 0), as well as the positive fixed point $(N^*, (1 - d)N^*)$, for $0 \le d < 1$ and $0 < N^* < 1$ in model (3).

Theorem.   The coexistence fixed point (N^*, P^*) exists and is unique if $s < 1/\beta$. Otherwise, there are either one or at most two positive fixed points.

Proof The solution of the following system gives the positive fixed point:

$$0 = r(1 - N^*)e^{-(\beta/1 + sN^*)} - a(1 - d)P^*$$
$$0 = aP^*((1 - d)N^* - P^*)\left(\frac{P^*}{m + P^*}\right). \tag{4}$$

The second equation of the system is solvable if $(1 - d)N^* = P^*$. By substituting this value into the first equation, we obtain

$$0 = r(1 - N^*)e^{-(\beta/1 + sN^*)} - a(1 - d)^2N^*. \tag{5}$$

Let $f(N) = r(1 - N)e^{-(\beta/1 + sN)}$ and $g(N) = a(1 - d)^2N$ on $N \in [0, 1]$. By the extreme value theorem, $f(N)$ must attain its maximum and minimum values on [0, 1].

Now, there are two roots that make $f'(N) = 0$, which are $\dot{N}_1 = \frac{-2s - \beta s - \sqrt{\beta s}\sqrt{4 + \beta + 4s}}{2s^2}$ and $\dot{N}_2 = \frac{-2s - \beta s + \sqrt{\beta s}\sqrt{4 + \beta + 4s}}{2s^2}$. It is obvious that $\dot{N}_1 < 0$ for all $\beta > 0$ and $s > 0$, so $\dot{N}_1$ is not in the domain [0, 1]. For $\dot{N}_2$, we have
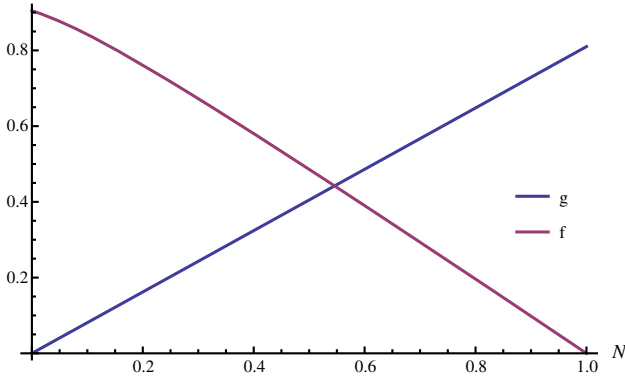
Figure 1. Positive fixed point for the case $s < \frac{1}{\beta}$ if $\beta = 0.1$, $a = 1$, $r = 1$, $s = 5$ and $d = 0.1$.

$$\begin{cases} \dot{N}_2 = 0 & s = \dfrac{1}{\beta} \\[2mm] \dot{N}_2 < 0 & s < \dfrac{1}{\beta} \\[2mm] 0 < \dot{N}_2 < 1 & s > \dfrac{1}{\beta}. \end{cases}$$

Hence, for $s \leq 1/\beta$, there is no interior critical point. The boundary values are $f(0) = e^{-\beta} r$ and $f(1) = 0$. If $s \leq 1/\beta$, then $f'(x) < 0$, $f''(x) < 0$. Thus, f is a decreasing concave down function that takes its maximum value at 0 and the minimum value at 1. Furthermore, because $g(0) = 0 < f(0)$, f cannot be below the linear function g, which implies that they should intersect. The function $g(N)$ is linear with a positive slope $a(1 - d)^2$. Then $f(N)$ and $g(N)$ intersect exactly once if $s < 1/\beta$. If $s > 1/\beta$, then $\dot{N}_2$ is a critical point. We have $f''(\dot{N}_2) < 0$, so f attains its maximum value at $\dot{N}$.

Under the condition $s > 1/\beta$, the following hold:

$$\begin{array}{ll} f'(N) > 0 & \text{if } 0 < N < \dot{N}_2 \\ f'(N) = 0 & \text{if } N = \dot{N}_2 \\ f'(N) < 0 & \text{if } \dot{N}_2 < N < 1. \end{array}$$
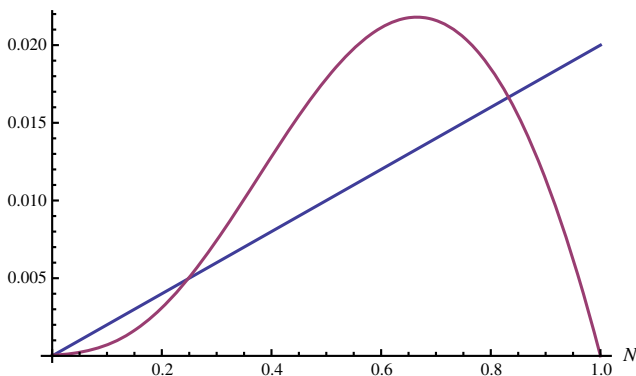
As a result $f(N)$ can intersect with the linear function more than once. $\qquad\square$

The numerical simulations for this theorem are shown in figures 1 and 2.

Stability analysis of the fixed points: (0, 0), (1, 0) and (N^*, P^*). The Jacobian matrix of the system (3) is given by

$$J = \begin{pmatrix} Q(N,P) & a(-1+d)N \\ -\dfrac{a(-1+d)P^2}{m+P} & \Phi(N,P) \end{pmatrix},$$

where

$$Q(N,P) = 1 - a(1-d)P + e^{-(\beta/1+Ns)}(1-N)r \\ - e^{-(\beta/1+Ns)}Nr + \frac{e^{-(\beta/1+Ns)}(1-N)Nrs\beta}{(1+Ns)^2},$$

and

$$\Phi(N,P) = 1 - \frac{a((1-d)N - P)P^2}{(m+P)^2} \\ + \frac{2a((1-d)N - P)P}{m+P} - \frac{aP^2}{m+P}.$$

Hence, we obtain

$$J(0,0) = \begin{pmatrix} 1 + re^{-\beta} & 0 \\ 0 & 1 \end{pmatrix},$$

with the eigenvalues $\lambda_1 = 1 + re^{-\beta} > 1$ and $\lambda_2 = 1$. Thus (0, 0) is unstable fixed point.

The Jacobian matrix at (1, 0) is

$$J(1,0) = \begin{pmatrix} 1 - re^{-(\beta/1+s)} & -a(1-d) \\ 0 & 1 \end{pmatrix}.$$

Since the eigenvalues are $\lambda_1 = 1 - re^{-(\beta/1+s)}$ and $\lambda_2 = 1$, the point (1, 0) is a non-hyperbolic fixed point, and its stability changes such that:
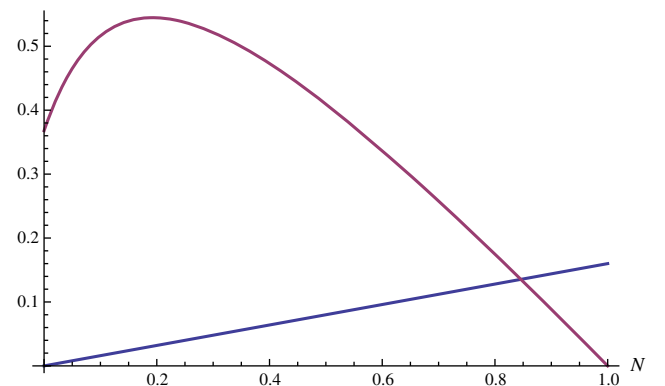

Figure 2. Positive fixed point(s) for the case $s > \frac{1}{\beta}$; for $\beta = 10$, $a = 2$, $r = 1$, $s = 4$ and $d = 0.9$, there are two positive fixed points. For $\beta = 1$, $a = 2$, $r = 1$, $s = 8$ and $d = 0.6$, there is one positive fixed point.

(i) If $\beta/(1+s) < \ln(r/2)$, then $|\lambda_1| > 1$, and $(1, 0)$ is not stable.

(ii) If $\beta/(1+s) = \ln(r/2)$, then $|\lambda_1| = |\lambda_2| = 1$, and the stability cannot be analyzed via current methods.

(iii) If $\beta/(1+s) > \ln(r/2)$, then $|\lambda_1| < 1$, and the Center Manifold Theorem can be used.

Since our focus is to address the stability of the coexistence equilibrium, we present the application of the Center Manifold Theorem in the Appendix for the readers who are interested in the details of its derivation.

In order to find the stability conditions of the coexistence fixed point, we substitute $(1 - d)N^* = P^*$, and obtain

$$J(N^*, P^*) = \begin{pmatrix} G(N^*) & -abN^* \\ \dfrac{ab^3N^{*2}}{m + bN^*} & 1 - \dfrac{ab^2N^{*2}}{m + bN^*} \end{pmatrix},$$

where
$$G(N^*) = -ab^2N^*$$
$$+ \frac{F(N^*)\left(F(N^*)(1+N^*s)^2 - (2N^*-1)r(1+N^*s)^2 - (N^*-1)N^*rs\beta\right)}{(1+N^*s)^2}, \quad F(N^*) =$$
$e^{-(\beta/1+N^*s)}$ and $b = 1 - d$.

We will use the Trace-Determinant Plane Theorem in order to examine the stability. The positive fixed point (N^*, P^*) is stable if the Jacobian matrix at this point satisfies the following condition:

$$|\operatorname{tr} J| - 1 < \det J < 1$$

We find $\det(J(N^*, P^*)) = \frac{a^2b^4N^{*3} + G(N^*)(m + bN^*(1 - abN^*))}{m + bN^*}$, and $\operatorname{tr}(J(N^*, P^*)) = 1 + G(N^*) - \frac{ab^2N^{*2}}{m + bN^*}$.

(i) $\det J < 1$ if $G(N^*) < \frac{mbN^* - a^2b^4N^{*3}}{m + bN^*(1 - abN^*)}$

(ii) $\operatorname{tr} J < 1 + \det J$ if $G(N^*) < 1 + ab^2N^*$

(iii) $-1 - \det < \operatorname{tr} J$ if $G(N^*) > \frac{-2(m + bN^*) - a^2b^4N^{*3} - ab^2N^{*2}}{1 - m + bN^*(1 - abN^*)}$

Hence (N^*, P^*) is stable if the following inequalities are satisfied:

$$\frac{-2(m + bN^*) - a^2b^4N^{*3} - ab^2N^{*2}}{1 - m + bN^*(1 - abN^*)}$$
$$< G(N^*) < min\left(1 + ab^2N^*, \frac{mbN^* - a^2b^4N^{*3}}{m + bN^*(1 - abN^*)}\right)$$

4. Numerical simulations

In this section, we present the dynamic behavior of the system (3) about the positive fixed point under different parameter values. To compare the resulting models, phase-plane diagrams, time-series diagrams and bifurcation diagrams are given. Although there is no explicit solution of the equation $0 = r(1 - N^*)\exp(-\beta/(1 + sN^*)) - a(1 - d)^2N^*$, by giving numerical values to the parameters, the fixed point can be found approximately. By substituting this positive fixed point into the Jacobian matrix, the corresponding eigenvalues can also be found to decide the stability type of the model. The following tables represent these approximate values.

In table 1, it is assumed that $d = 0$, which means that no prey can escape from its predators without encountering them first. For different values of predator's mate limitation coefficient m, the behavior of the system is presented under the assumption $d = 0$, $a = 1$, $\beta = 1$, $s = 0.5$ and $r = 5$. For these values we have $s < 1/\beta$, so there is unique positive fixed point, which is approximately $(0.705, 0.705)$. The values of a, β, s, d and r are sufficient to find the coexistence fixed point approximately. However, in the Jacobian, there is also an Allee effect coefficient m, which does not affect the value of the point, but may affect the stability. If there is no mate limitation Allee effect ($m = 0$) or m is small enough, then the system exhibits spiral sink behavior. As m increases, the system begins to oscillate, but remains stable. Figures 3–5 consist of phase diagrams and time-series graphs associated with table 1. Additionally, in the tables below, we provide eigenvalues as reference, for which certain stability types are observed. For instance, as given in table 2, when $|\lambda_2| < 1$ and $\lambda_1 < -1$, we observe oscillatory saddle behavior.

In figures 3–5 we examine phase and time-series diagrams under various values of m, while the parameters $a = 1$, $\beta = 1$, $s = 0.5$, $r = 5$ and $d = 0$ are kept fixed, and the initials points are chosen as $N = 0.2$ and $P = 0.2$.

Table 2 and figures 6–8 show how the change of m affects the dynamic behavior of the system, while the parameters $a = 1$, $\beta = 1$, $s = 0.5$, $r = 5$ and $d = 0.5$ are kept fixed. The positive fixed point is an oscillatory saddle. The systems have a two-periodic stable cycle for all values of m, but the amplitude of the cycle of the predator decreases as m increases. The initial values are taken as $N = 0.2$ and $P = 0.2$.

Table 1. Effects of m with $a = 1$, $\beta = 1$, $s = 0.5$, $r = 5$ and $d = 0$

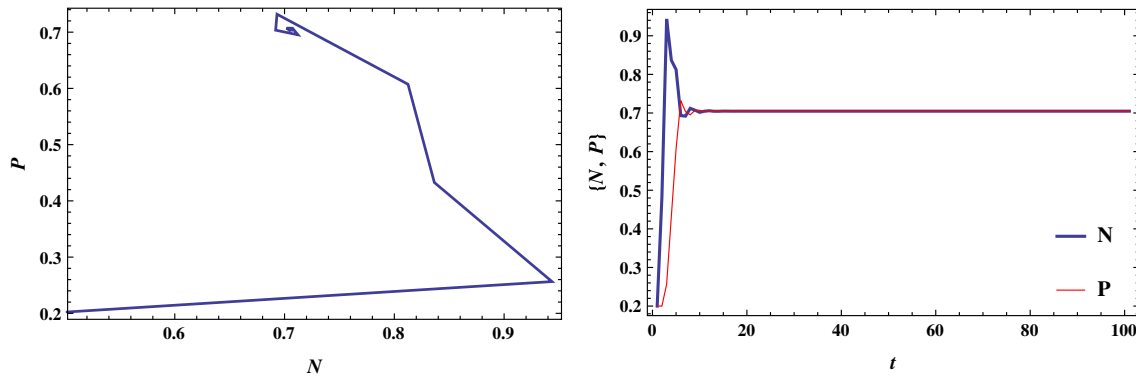| m	Positive fixed point	Eigenvalues	Stability type
0	(0.705, 0.705)	$\lambda_{1,2} = -0.125 \pm 0.565i$ with $|\lambda| = 0.82$	Spiral sink
0.4	(0.705, 0.705)	$\lambda_{1,2} = -0.002 \pm 0.127i$ with $|\lambda| = 0.18$	Spiral sink
0.5	(0.705, 0.705)	$\lambda_1 = 0.197$, $\lambda_2 = -0.155$	Oscillatory stable
1	(0.705, 0.705)	$\lambda_1 = 0.304$, $\lambda_2 = -0.231$	Oscillatory stable
5	(0.705, 0.705)	$\lambda_1 = 0.515$, $\lambda_2 = -0.353$	Oscillatory stable

Figure 3. Phase diagrams and time-series diagrams for $m = 0$.
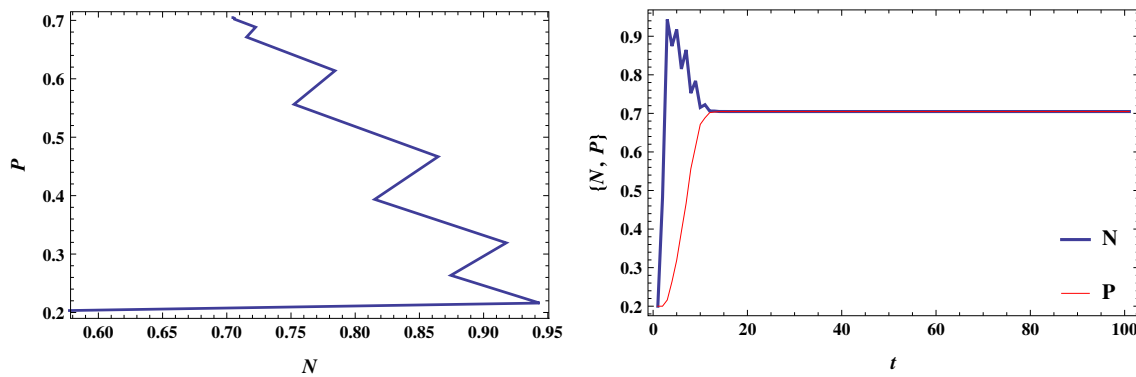

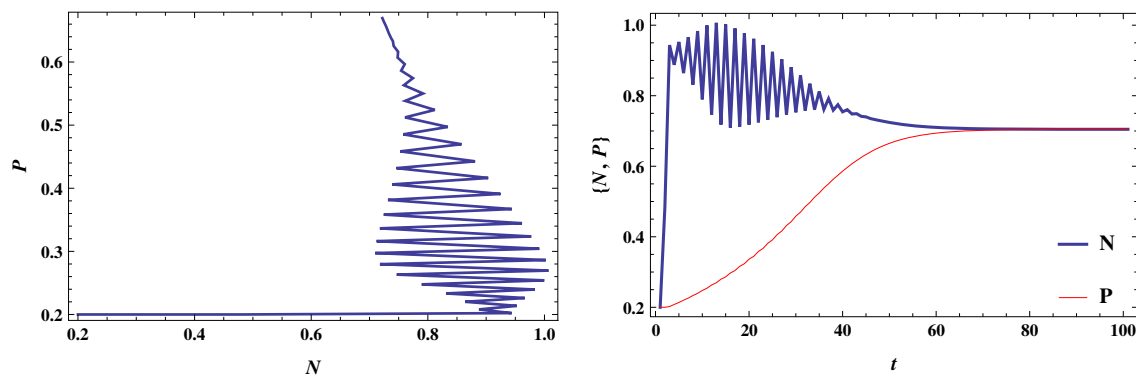**Figure 4.** Phase diagrams and time-series diagrams for $m = 0.5$.

Figure 5. Phase diagrams and time-series diagrams for $m = 5$.

Table 2. Effects of m with $a = 1$, $\beta = 1$, $s = 0.5$, $r = 5$ and $d = 0.5$

m	Positive fixed point	Eigenvalues	Stability type	2 periodic cycles
0	(0.91, 0.455)	$\lambda_1 = -1.178$, $\lambda_2 = -0.485$	Oscillatory saddle	{(0.72,0.46), (1.04,0.41)}
0.5	(0.91, 0.455)	$\lambda_1 = -1.214$, $\lambda_2 = -0.759$	Oscillatory saddle	{(0.7,0.44), (1.05,0.42)}
1	(0.91, 0.455)	$\lambda_1 = -1.223$, $\lambda_2 = 0.842$	Oscillatory saddle	{(0.7,0.44), (1.05,0.43)}
5	(0.91, 0.455)	$\lambda_1 = -1.234$, $\lambda_2 = 0.95$	Oscillatory saddle	{(0.7,0.43), (1.05,0.43)}

Table 3 and figures 9–11 show the effects of m when there is a high amount of refuge ($d = 0.8$). The other parameters are taken to be same as those in the previous tables.

Tables and diagrams given in this section show that when the value of d changes, the dynamic behavior changes, and the system doubles the periods of cycles. If $d = 0$, then the
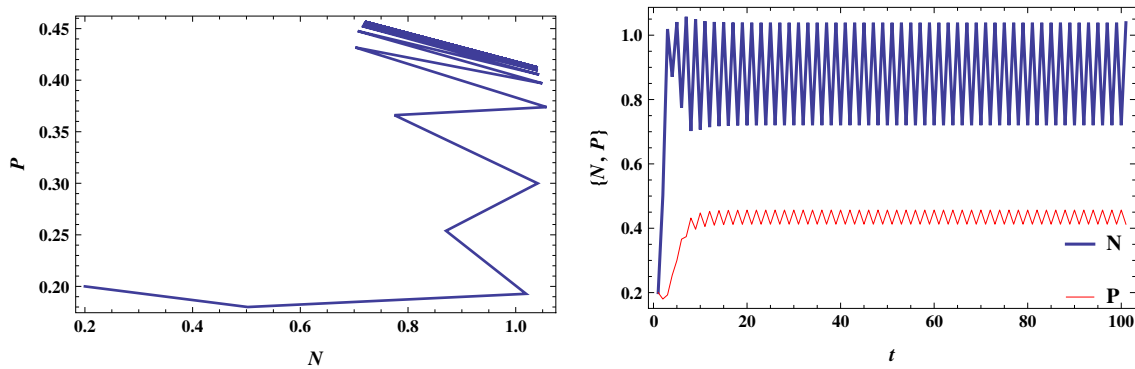
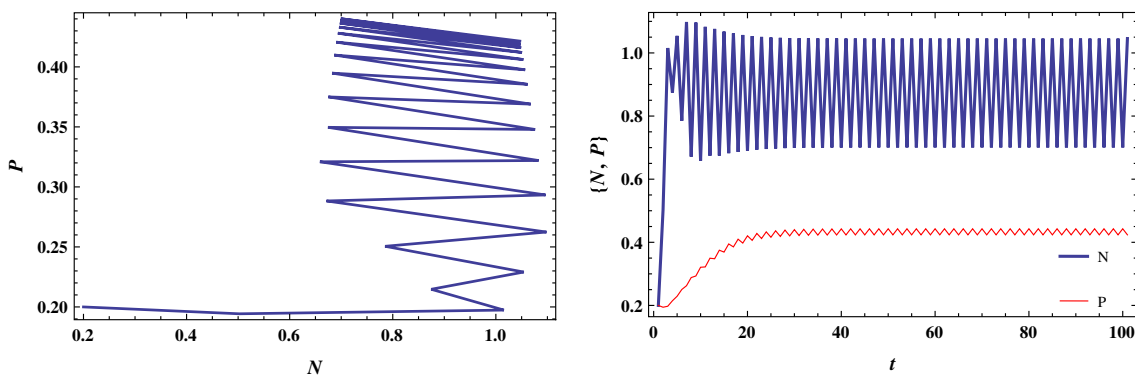**Figure 6.**   Phase diagrams and time-series diagrams for $m = 0$.

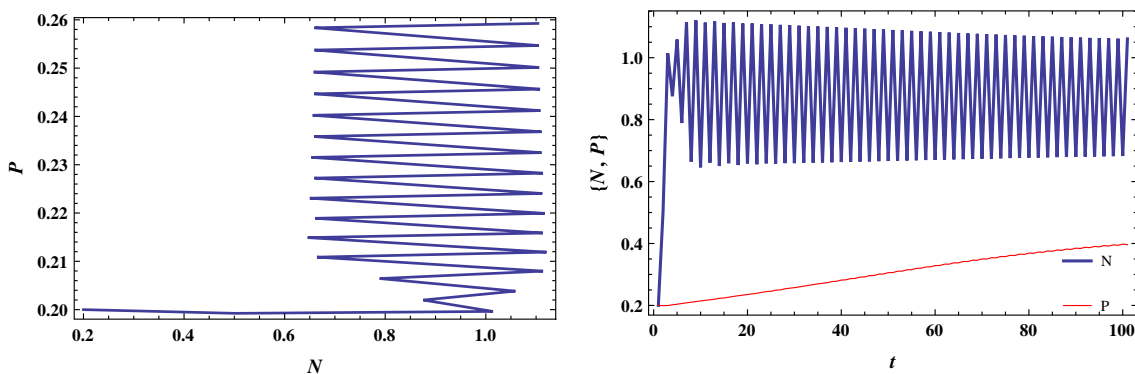**Figure 7.**   Phase diagrams and time-series diagrams for $m = 0.5$.

Figure 8.   Phase diagrams and time-series diagrams for $m = 5$.

Table 3.   Effects of m with $a = 1$, $\beta = 1$, $s = 0.5$, $r = 5$ and $d = 0.8$

m	Positive fixed point	Eigenvalues	Stability type	Four periodic cycle
0	(0.985, 0.197)	$\lambda_1 = -1.507$, $\lambda_2 = 0.8$	Oscillatory saddle	{(1.177,0.175), (0.58,0.186), (1.112,0.173), (0.728,0.181)}
0.5	(0.985, 0.197)	$\lambda_1 = -1.509$, $\lambda_2 = -0.943$	Oscillatory saddle	{(1.177,0.179), (0.579,0.181), (1.112,0.178), (0.728,0.18)}
5	(0.985, 0.197)	$\lambda_1 = -1.51$, $\lambda_2 = -0.99$	Oscillatory saddle	{(1.177,0.182), (0.579,0.183), (1.119,0.182), (0.728,0.183)}

positive fixed point is stable. With a moderate d value, there is a two-periodic cycle, while with a great value of d the period of the cycle is four. If the system has a cycle, then the positive fixed point loses its stability. The predator population oscillates, but the amplitude is so small that P^* seems stable. On the other hand, the magnitude of the oscillation is
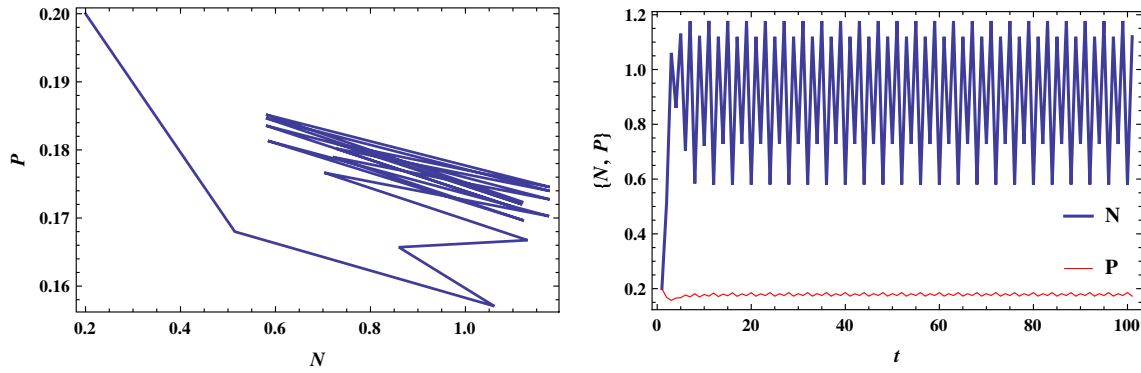
Figure 9. Phase diagrams and time-series diagrams for $m = 0$.
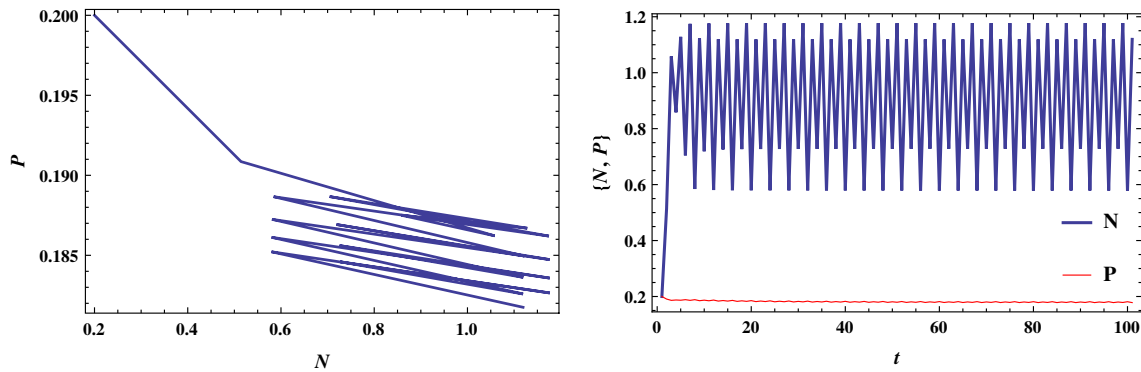

Figure 10. Phase diagrams and time-series diagrams for $m = 0.5$.
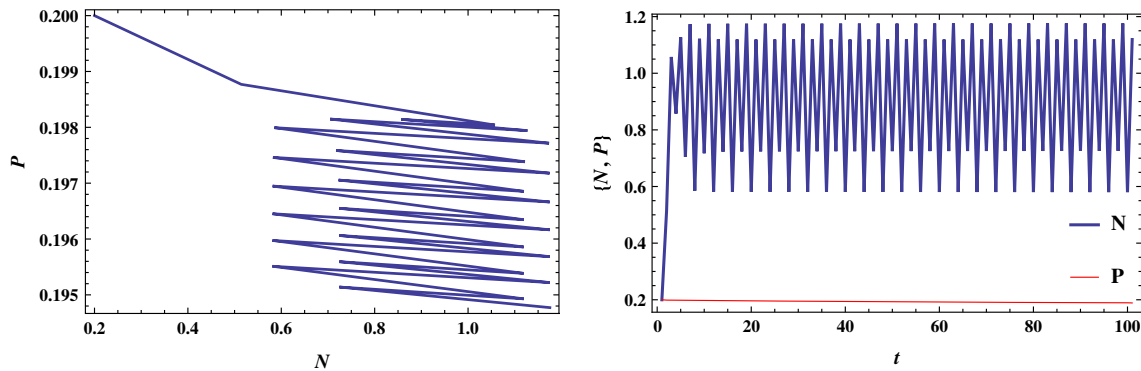

Figure 11. Phase diagrams and time-series diagrams for $m = 5$.

greater for prey, hence N^* is unstable. As a result, the fixed point (N^*, P^*) is a saddle fixed point. As m increases, the oscillation amplitude of the predator decreases. The system goes through a period doubling bifurcation with respect to d, and the bifurcation plots are shown in figure 12 at the values $a = 1$, $\beta = 1$, $s = 0.5$ and $r = 5$.

5. Concluding remarks

In this paper a new discrete predator–prey model, namely model (3), is proposed. This model contains a new predator saturation term in addition to the mate limitation

of predators. Model (3) extends the models that are commonly used to study prey–predator dynamics via Allee effects. It contains the refuge effect term with and without encounters with the predator. We have studied the model analytically, and performed numerical simulations to study its stability and bifurcation behavior. Our findings indicate an interesting fact that the equilibria, even the predator value in the equilibria, depend on the dynamics of prey and the interaction between predator and prey. Biologically this corresponds to the case where the predator population is closely defined by the prey. As a result, the effects added to prey dominantly impact the model. We have also discussed the biological relevance of
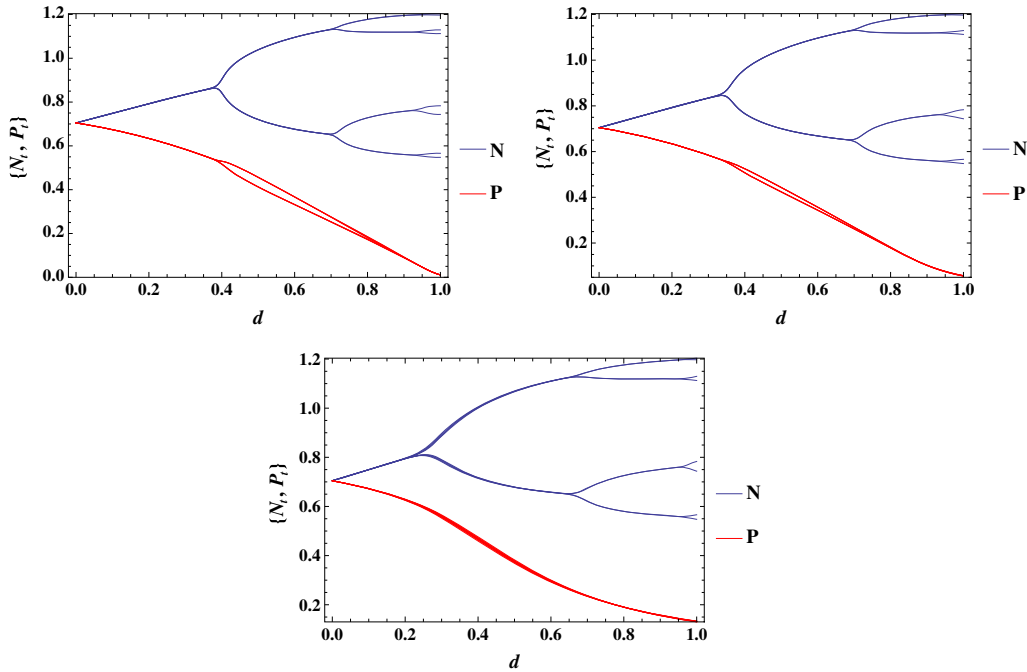
Figure 12. The bifurcation diagrams for $m = 0$, $m = 0.5$ and $m = 5$, respectively.
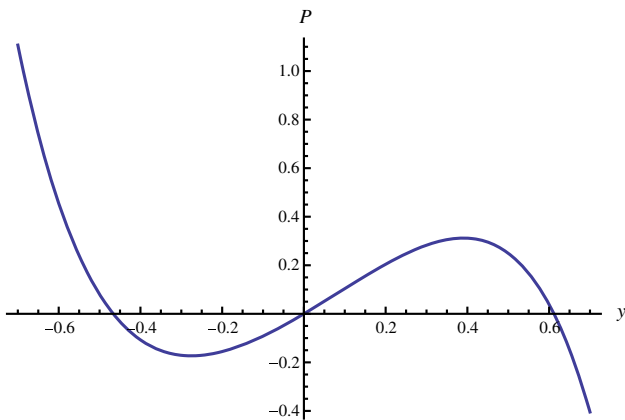

Figure 13. The map P on the semistable invariant manifold $x = h(y)$ for $\beta = 4$, $a = 2$, $r = 5$, $s = 1$, $m = 2$ and $d = 0.4$.

the model. The analytical and numerical results indicate that the effects of prey refuge and Allee effects for pattern formulation are substantial. We believe this understanding will enrich the dynamics of the effects on the predator–prey systems. The numerical simulations have shown that our system is capable of generating complex temporal dynamics. We have also presented a rigorous proof related to the general behavior of the dynamical equation depending on the conditions on the parameter space. Specifically, we have obtained the existence and uniqueness of positive fixed points. We have also examined the effects of the stability of the origin, the extinction fixed point and the positive fixed point on the dynamics of the model.

Appendix

If a non-hyperbolic map is defined on $\mathbb{R}^2$, then its dynamics may be analyzed by studying the dynamics on an associated one-dimensional center manifold M_c (Elaydi 2008). This theorem is applicable only for the fixed point (0,0). Hence, we get the following new system by setting $x_t = N_t - 1$ and $y_t = P_t$:

$$
\begin{aligned}
x_{t+1} &= x_t - e^{-(\beta/1+s(1+x_t))}rx_t(1+x_t) - a(1-d)(1+x_t)y_t \\
y_{t+1} &= y_t + \frac{a((1-d)(1+x_t) - y_t)y_t^2}{m+y_t}.
\end{aligned}
\tag{6}
$$

Let J^* be the Jacobian matrix of the system (6). Then

$$
J^*(0,0) = \begin{pmatrix} 1 - re^{-(\beta/1+s)} & -a(1-d) \\ 0 & 1 \end{pmatrix}
$$

Rewriting system (6), we obtain

$$
\begin{aligned}
x_{t+1} &= (1 - re^{-(\beta/1+s)})x_t - ay_t(1-d) + \tilde{f}(x_t, y_t) \\
y_{t+1} &= y_t + \tilde{g}(x_t, y_t),
\end{aligned}
\tag{7}
$$

where

$$
\tilde{f}(x, y) = x(re^{-(\beta/1+s)} - re^{-(\beta/1+s+sx)}(1+x) + a(-1+d)y),
$$

and

$$\tilde{g}(x,y) = \frac{a((1-d)(1+x)-y)y^2}{m+y}.$$

$$P(y) \approx y - \frac{a(-1+d)y^2}{m} - \frac{a\left(a(-1+d)^2 m + k(1-d+m)r\right)y^3}{km^2 r}$$
$$+ \frac{a\left(1-d+m+(a(-1+d)^2 m/kr) - (a^2(-1+d)^3 m\left((1+s)^2 - ms\beta\right)/k^2 r^2(1+s)^2)\right)y^4}{m^3}.$$

By using the Taylor series expansion of $e^{-(\beta/1+s+sx)}$ at the point $x = 0$, we approximate

$$e^{-(\beta/1+s+sx)} \approx e^{-(\beta/1+s)} + \frac{ae^{-(\beta/1+s)}sx}{(1+s)^2}$$
$$+ \frac{\beta e^{-(\beta/1+s)}(-2+\beta-2s)s^2 x^2}{2(1+s)^4} + O(x^3)$$

For simplification, let $k = e^{-(\beta/1+s)}$. Then

$$\tilde{f}(x,y) \approx x\left(kr - \left(k + \frac{\beta ksx}{(1+s)^2} + \frac{\beta k(-2+\beta-2s)s^2 x^2}{2(1+s)^4}\right)\right)$$
$$(1+x) + a(-1+d)y.$$

Since the invariant manifold is tangent to the corresponding eigenspace by the Invariant Manifold Theorem, assume that the map h takes the form

$$h(y) = \frac{a(d-1)}{rk}y + c_1 y^2 + c_2 y^3 + O(y^4).$$

To compute c_1 and c_2, the following functional equation should be solved:

$$h(y + \tilde{g}(h(y),y)) \approx (1 - re^{-(\beta/1+s)})h(y) - a(1-d)y$$
$$+ \tilde{f}(h(y),y).$$

We have

$$c_1 \approx -\frac{a^2(-1+d)^2(-1-2s-s^2+ms\beta)}{k^2 mr^2(1+s)^2},$$

and

$$c_2 \approx \frac{a^2(-1+d)}{2k^3 m^2 r^3(1+s)^4}(2k(1-d+m)r(1+s)^4$$
$$+ a(-1+d)^2(4(1+s)^4 + 2ms(1+s)$$
$$(-4+(-4+m)s)\beta + 3m^2 s^2 \beta^2)).$$

This leads to the equation

We have $P'(0) = 1$ and $P''(0) = 2a(1-d)/m > 0$ for $a > 0$, $m > 0$ and $d \in [0,1)$. Hence, by Theorem 1.5 in Elaydi (2008), (1, 0) is a semistable fixed point if $\beta/(1+s) > \ln(r/2)$ (See figure 13).

References

Celik C and Duman O 2009 Allee effect in a discrete time predator-prey system. *Chaos, Solitons Fractals.* **40** 1956–1962

Courchamp F, Berec L and Gascoigne J 2008 *Allee effects in ecology and conservation* (Oxford: Oxford University Press)

Elaydi S 2008 *Discrete chaos: With applications in science and engineering* 2nd edition (Boca Raton: Chapman & Hall/CRC)

Hassell MP 1978 *The dynamics of arthropod predator-prey systems* (Princeton, NJ: Princeton University Press)

Hassell MP and May RM 1973 Stability in insect host-parasite models. *J. Anim. Ecol.* **42** 693–726

Hassell MP, Lawton JH and Beddington JR 1976 The components of arthropod predation: I. The prey death-rate. *J. Anim. Ecol.* **45** 135–164

Jana D 2013 Chaotic dynamics of a discrete predator-prey system with prey refuge. *Appl. Math. Comput.* **224** 848–865

Ma Z, Li W, Zhao Y, Wang W, Zhang H and Li Z 2009 Effects of prey refuges on a predator–prey model with a class of functional responses: The role of refuges. *Math. Biosci.* **218** 73–79

McNair JN 1986 The effects of refuges on predator-prey interactions—a reconsideration. *Theor. Popul. Biol.* **29** 38–63

Rana S, Bhowmick AR and Bhattacharya S 2014 Impact of prey refuge on a discrete time predator-prey system with Allee effect. *Int. J. Bifurcation Chaos* **24** 1450106

Scheuring I 1999 Allee effect increases the dynamical stability of populations. *J. Theor. Biol.* **199** 407–414

Schreiber SJ 2003 Allee effects, extinctions, and chaotic transients in simple population models. *Theor. Popul. Biol.* **64** 201–209

Taylor RJ 1984 *Predation* (NY: Chapman and Hall)

Ufuktepe U, Kapcak S and Akman O 2013 Stability and invariant manifold for a predator–prey model with Allee effect. *Adv. Differ. Equ.* **1** 1–8

Wang G, Liang X-G and Wang F-Z 1999 The competitive dynamics of populations subject to an Allee effect. *Ecol. Model.* **124** 183–192

Corresponding editor: N. G. PRASAD